

Bismuth charge disproportionation in semiconducting $\text{BaPb}_x\text{Bi}_{1-x}\text{O}_3$ studied by infrared reflection spectroscopy

This article has been downloaded from IOPscience. Please scroll down to see the full text article.

2007 J. Phys.: Condens. Matter 19 266223

(<http://iopscience.iop.org/0953-8984/19/26/266223>)

View [the table of contents for this issue](#), or go to the [journal homepage](#) for more

Download details:

IP Address: 129.252.86.83

The article was downloaded on 28/05/2010 at 19:37

Please note that [terms and conditions apply](#).

Bismuth charge disproportionation in semiconducting $\text{BaPb}_x\text{Bi}_{1-x}\text{O}_3$ studied by infrared reflection spectroscopy

Javed Ahmad^{1,2}, Hisayuki Yamanaka¹ and Hiromoto Uwe¹

¹ Institute of Materials Science, University of Tsukuba, Tennoudai, Tsukuba, Ibaraki 305-8573, Japan

² Department of Physics, Bahauddin Zakariya University, Multan 60800, Pakistan

E-mail: dr.j.ahmad@gmail.com

Received 27 February 2007, in final form 31 May 2007

Published 18 June 2007

Online at stacks.iop.org/JPhysCM/19/266223

Abstract

The infrared reflectivity spectra of semiconducting $\text{BaPb}_x\text{Bi}_{1-x}\text{O}_3$ single crystals are measured. From the oscillator strength of the bismuth charge-disproportionation mode we compute the compositional dependence of the Born and Szigeti effective-charge difference between two inequivalent bismuth sites. The Szigeti effective-charge decreases and is found to become zero as the Pb doping approaches the critical value of the semiconductor–metal transition. This behaviour is associated with the Pb composition induced closing of the indirect energy gap, which takes place prior to the direct gap. It further demonstrates that the long-range order of the bismuth charge disproportionation completely vanishes in the metallic phase. It is found that a strong dynamical charge transfer takes place along the bismuth–oxygen–bismuth bond enhanced by the lattice vibration. The results are compared with those of $\text{Ba}_{1-x}\text{K}_x\text{BiO}_3$ system.

1. Introduction

Over the past several years the alloy systems $\text{BaPb}_x\text{Bi}_{1-x}\text{O}_3$ (BPBO) and $\text{Ba}_{1-x}\text{K}_x\text{BiO}_3$ (BKBO) have attracted tremendous interest due to their exhibition of interesting physical phenomena, namely superconductivity with a transition temperature (T_c) comparable to those of high- T_c cuprate superconductors, in spite of the low density of states at the Fermi level, and the composition-induced semiconductor–metal (SM) transition. The parent compound of both BPBO and BKBO, i.e. BaBiO_3 (BBO), is a three-dimensional Peierls semiconductor with a body-centred monoclinic lattice symmetry arising from a cubic perovskite structure due to distortions of (1) the tilting or rotation around the [100] and [110] axes of oxygen octahedra and (2) the breathing mode that disproportionates the charge on bismuth atoms [1–4]. The latter produces an ordered arrangement of $\text{Bi}^{(4-\delta)+}$ and $\text{Bi}^{(4+\delta)+}$ ions, i.e. a commensurate charge-density wave (CDW). Although disproportionation of Bi^{4+} into two inequivalent $\text{Bi}^{(4-\delta)+}$ and

$\text{Bi}^{(4+\delta)+}$ ions is considered to play a key role in the novel physical properties of BBO and its alloys, the existence and, in particular, the extent of the charge disproportionation, i.e. the value of δ , is still controversial. For example, Namatame *et al* [5] could not find two Bi sites in their x-ray photoemission spectrum for the Bi 4f level. On the other hand, neutron diffraction experiments revealed Bi ions occupying two crystallographically inequivalent sites with significantly different Bi–O bond lengths [2, 6, 7]. The existence of two sites is also supported by extended x-ray absorption fine structure (EXAFS) and optical studies [8, 9]. These results are also supported by x-ray photoemission [10] and x-ray absorption near-edge structure spectroscopy [11], but demonstrate a minimal charge transfer between the two Bi sites consistent with the defect simulation studies [12] and band-structure calculation [13, 14]. The latter predicts a charge difference as small as $0.01e$.

On Pb substitution at the electronically active Bi sites, the doped BBO undergoes a series of structural phase transitions [3] and exhibits semiconducting behaviour up to a critical concentration $x_c = 0.65$ of the SM transition. In the metallic phase, the BPBO shows superconductivity with a maximum $T_c = 13$ K for $x = 0.75$ [15]. In the previous optical studies regarding the origin of the insulating behaviour and the mechanism of the SM transition in BPBO, a much earlier work of Uchida *et al* [16] revealed four residual bands in the reflectivity spectrum of BBO. They found that the oscillator strength of the Bi charge disproportionation mode decreases appreciably and that the three high-frequency modes split, which is indicative of what is called two-mode behaviour, with increasing Pb concentration. Their evidence for the charge disproportionation was striking, but the decreasing oscillator strength with Pb substitution was not connected to the decreasing CDW amplitude, since the estimated transverse effective charge difference between two inequivalent Bi sites was too big due to a strong dynamical charge transfer effect. Recently, for BKBO, where the SM transition takes place at $x_c = 0.3$ and superconducting BKBO reaches a maximum $T_c = 30$ K for $x = 0.4$ [17, 18], Nishio and Uwe [19] measured the optical phonon spectra to estimate the doping dependence of the Born and Szigeti effective charges for the disproportionation mode. The Szigeti effective charge, which is acted on by the local field, was found to be much smaller than the Born effective charge, despite still recognizing the strong dynamical charge transfer effect. Furthermore, the Szigeti charge was found to decrease more smoothly to the SM transition with doping than the Born charge. It is, therefore, required to revisit the phonon spectra of BPBO in order to evaluate the doping dependence of the effective charges to get information on the SM transition.

Our recent optical reflectivity measurements demonstrated that the mechanism of the persistent semiconducting state was the formation of small bipolarons and thermally excited small hole and small electron polarons [20–23]. In the optical transmission experiments, the indirect-exciton structure in the mid-infrared region consistent with the results of the transport experiment [24, 25] was found for BBO [26], BPBO [27] and BKBO [28].

The purpose of this paper is to investigate quantitatively the doping effect of the Bi charge disproportionation and discuss the SM transition along with the behaviour of electronic excitation through the indirect energy gap in the strong electron–phonon interaction system BPBO. Following our recent success of the preparation of single crystals, here we report on the optical reflectivity spectra in the infrared frequency range at various temperatures between 20 and 300 K for the Pb doping covering the whole semiconducting region.

2. Experiment

Single crystals of BPBO were prepared by melting followed by slow cooling of a stoichiometric mixture of Ba_2CO_3 (99.9%), Pb_3O_4 (99.99%) and Bi_2O_3 (99.99%). The powders of the starting

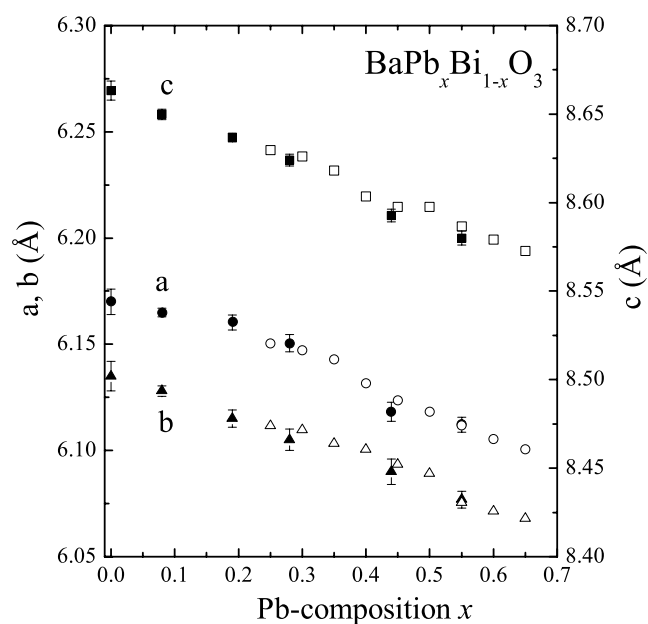


Figure 1. The compositional dependence of the unit cell parameters of single crystals of BPBO (solid symbols). The open symbols are those estimated by Marx *et al* [3] using neutron powder diffraction data.

materials were mixed for 1 h in an agate mortar to ensure uniformity, placed in an Al₂O₃ crucible and heated at 1080 °C for 2 h in flowing ultrahigh-purity nitrogen. Heating up to such a high temperature ensured full reaction while avoiding the loss of lead. The melt was then cooled slowly (2 °C h⁻¹) to 1000 °C, kept at this temperature for 2 h, and again cooled slowly (6 °C h⁻¹) to 450 °C before switching off the furnace to allow it to reach room temperature. Without taking out it of the furnace, the melt was then annealed at 300 °C for 3 h in flowing oxygen. Large-size crystals (the largest one was 8 × 8 × 2 mm³) were found at the bottom of the crucible. The decrease in size of the crystals and the change in its colour from gold to dark purple (almost black) was noticed with an increase in the Pb concentration x . Thus, for $x = 0.55$, the crystal was found to be smaller in size inside the crucible. The Pb concentration was determined by an electron-probe microanalysis (EPMA). Part of the crystals were ground to powder form for x-ray diffraction measurements, which were carried out using Cu K α ($\lambda = 1.5418$ Å) radiation. The lattice parameters calculated from the diffraction patterns assuming the orthorhombic structure are shown in figure 1. The lattice parameters decrease continuously with x and the values almost overlap those estimated by Marx *et al* [3] using neutron powder diffraction experiments. All the single crystals were cut into parallelepipeds of size equal to or larger than 4 × 4 × 1 mm³ with large (100) surfaces. One of the surfaces was polished to a mirror-like surface using Al₂O₃ powder 0.05 μ m in size, which was used for optical reflectivity measurements. The reflectivity spectra were measured at $\sim 11^\circ$ incidence by using the Fourier-transform infrared spectrometer in a frequency range of 50–7500 cm⁻¹. The spectra were measured at various temperatures between 20 and 300 K. The absolute value of the reflectivity was determined compared with that of an evaporated Au film measured with the same optical alignment. Further details of experimental setup and procedure used for recording the reflectivity spectra can be found elsewhere [22].

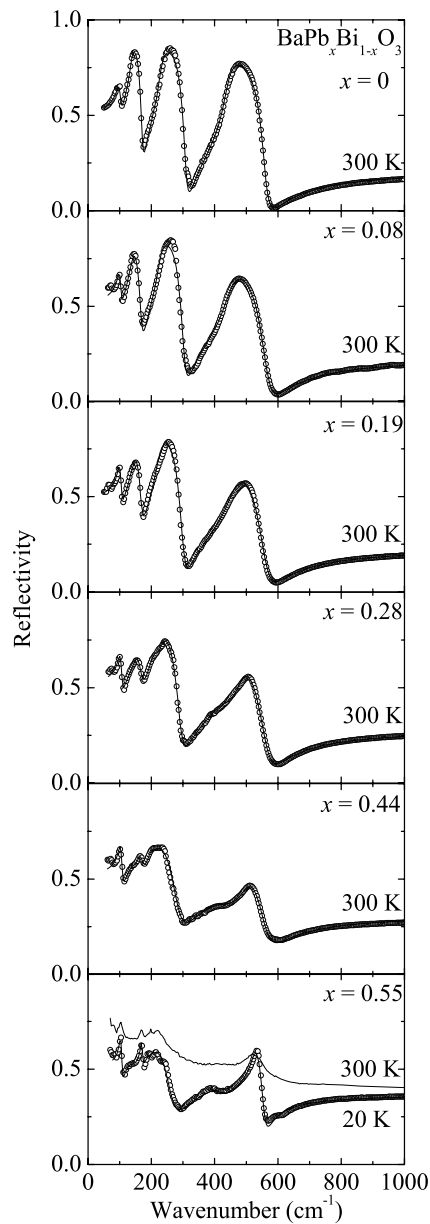


Figure 2. The reflectivity spectra of BPBO (open circles). The lines are the fit of the Lorentz-oscillator model to the spectra. Note the difference in the reflectivity spectrum at 300 and 20 K for $x = 0.55$ (lower panel) where the spectrum at 300 K also involves the absorption due to thermally excited carriers.

3. Results and discussion

The reflectivity spectra of BPBO for $x = 0, 0.08, 0.19, 0.28, 0.44$ and 0.55 in the frequency range $50\text{--}1000\text{ cm}^{-1}$ are shown in figure 2. As Uchida *et al* [16] reported, we have also observed at least four main bands but with comparatively greater intensity for each spectrum, which are the stretching mode of the Bi–O bond, the ferroelectric mode, the Bi-charge

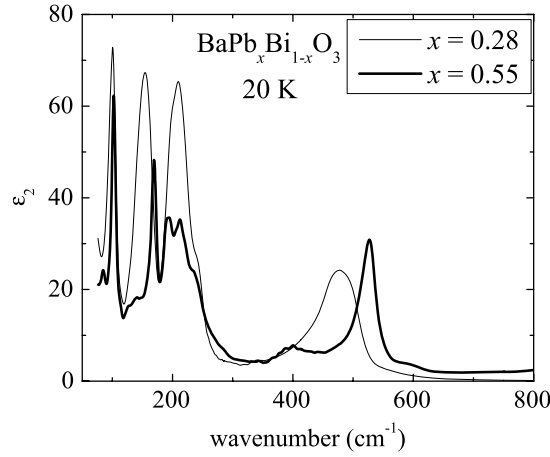


Figure 3. Imaginary dielectric constant, ϵ_2 obtained from Kramers–Kronig transformation of corresponding reflectivity spectra for $x = 0.28$ (thin line) and 0.55 (thick line) at 20 K. The splitting of three high-frequency TO modes can clearly be seen for $x = 0.55$.

disproportionation mode and the Last mode, in order of decreasing frequency [29–31]. For $x > 0.28$, the three high-frequency modes begin to split, which is consistent with what is called a two-mode behaviour observed for the BPBO system. Besides, as Pb doping increases, the reflectivity spectrum of phonons seems to superimpose on the background absorption that appears, because of thermally excited carriers due to narrowing of the band gap. As a result, it becomes difficult to distinguish the phonon modes. At 300 K, we noticed that, while phonon modes were distinguished for $x = 0.28$, these were not become clearly observable for more heavily doped samples with a Pb concentration near to the x_c of the SM transition, as can typically be seen for $x = 0.55$. In the case of $x = 0.55$, we have therefore used the reflectivity spectrum at 20 K, where the phonon modes can clearly be seen for the analysis, thereby excluding the contribution from the thermally excited carriers.

Concerning two-mode behaviour of BPBO system, the splitting of transverse optic (TO) modes can be best viewed from the imaginary part of the dielectric constant ϵ , i.e. the ϵ_2 spectra, which exhibits peaks at the TO mode frequencies. Figure 3 represents the ϵ_2 for $x = 0.28$ and 0.55 at the lowest measured temperature 20 K to see the available TO modes clearly. It can be seen that the three high-frequency modes split for $x = 0.55$. The new modes represent the vibration of Pb-sublattice and emerge on sufficient Pb doping at the Bi sites. The splitting of TO modes is almost absent for lightly doped $x \leq 0.28$ sample. Uchida *et al* [16] also found that the TO modes start to split for $x > 0.28$. In pseudobinary mixed crystals of form $A_{1-x}B_xC$, the one-mode behaviour initially exhibited by the crystals for smaller x changes to two-mode behaviour on increasing x [32]. It seems that the BPBO crystals show a similar property. Therefore, we conclude that the BPBO system exhibits two-mode behaviour. However, this is in contrast to what Lobo and Gervais [33] reported for their ceramic sample, with Yb doped at the Bi sites, for which they did not find mode splitting and claimed that the system showed single-mode behaviour.

We have analysed the reflectivity spectra using the Lorentz-oscillator model, in which the $\epsilon(\omega)$ is defined as

$$\epsilon(\omega) = \epsilon_\infty + \sum_j \frac{\omega_{\text{TO}}^2(j)S_j}{\omega_{\text{TO}}^2(j) - \omega^2 - i\omega\gamma_j} \quad (1)$$

Table 1. The parameters extracted from fitting equation (1) to the reflectivity spectra of $\text{BaPb}_x\text{Bi}_{1-x}\text{O}_3$ for various x at 300 K except for $x = 0.55$, which is at 20 K.

	x					
	0	0.08	0.19	0.28	0.44	0.55
ω_1 (cm ⁻¹)	439	444	460	477	507	526
ω'_1 (cm ⁻¹)	—	—	—	—	427	412
ω_2 (cm ⁻¹)	230	227	223	217	213	213
ω'_2 (cm ⁻¹)	—	—	—	—	198	193
ω_3 (cm ⁻¹)	137	138	146	154	165	169
ω'_3 (cm ⁻¹)	—	—	—	—	145	139
ω_4 (cm ⁻¹)	98	99	99	100	102	103
S_1	3.0	3.4	2.9	3.4	1.7	1.7
S'_1	—	—	—	—	2.0	0.6
S_2	7.6	8.4	7.9	10.3	12	10.4
S'_2	—	—	—	—	1.2	0.4
S_3	14.4	12.4	9.4	7.6	3	1.4
S'_3	—	—	—	—	2	1.5
S_4	6.1	6.1	6.2	6.4	6.4	4.0
γ_1 (cm ⁻¹)	31	54	59	70	63	28
γ'_1 (cm ⁻¹)	—	—	—	—	150	58
γ_2 (cm ⁻¹)	21	22	27	39	61	65
γ'_2 (cm ⁻¹)	—	—	—	—	18	20
γ_3 (cm ⁻¹)	13	19	22	26	20	7
γ'_3 (cm ⁻¹)	—	—	—	—	31	35
γ_4 (cm ⁻¹)	13	10	11	11	11	8
ϵ_∞	7.3	8.1	8.0	10.3	12.4	16.9

where ϵ_∞ is the high-frequency dielectric function, $\omega_{\text{TO}}(j)$ is the transverse optical phonon frequency, S_j is the oscillator strength, and γ_j is the phonon-damping factor of the j th TO mode. Since the phonon splitting is not large enough at room temperature for $x \leq 0.28$, we use four Lorentzians in order to investigate the essential features of the main phonon modes. However, for $x > 0.28$, three high-frequency phonon modes split due to the different resonant frequencies of the Pb and Bi sublattices. Therefore, three additional Lorentzians have been used to reproduce the experimental spectra. The reflectivity spectra calculated using equation (1) are shown in figure 2, along with the experimental spectra, and the deduced fit parameters are tabulated in table 1.

On comparing these values given in table 1 with those estimated for BKBO [19], we find that the values of unprimed ω s coincide well with the TO-phonon frequencies for the one-mode-type BKBO. The frequencies for the three highest modes, i.e. the stretching, ferroelectric and disproportionation modes, are determined mainly by the covalent-bond force between (Bi, Pb) and O, since essentially covalent bonding is predicted theoretically [14, 17] and observed experimentally [34]. The splitting of the modes is due to the difference in covalent bonds between the Bi and O ions and between Pb and O ions, as also pointed out in [19] for BKBO. The one-mode behaviour of the Last mode is due to the fact that the distance between the (Bi, Pb) and O remains constant in the relative motion of Ba and the (Bi, Pb)O₃ octahedron. The increase in the frequencies of mainly two modes, i.e. mode 1 and 3, with Pb concentration suggests that the bond length of the (Bi,Pb)-O bond decreases with increasing Pb concentration. This is consistent with the observed decrease in the lattice parameters, as shown in figure 1, and the decrease in the volume of the pseudo-cubic unit cell [35] with increasing Pb concentration.

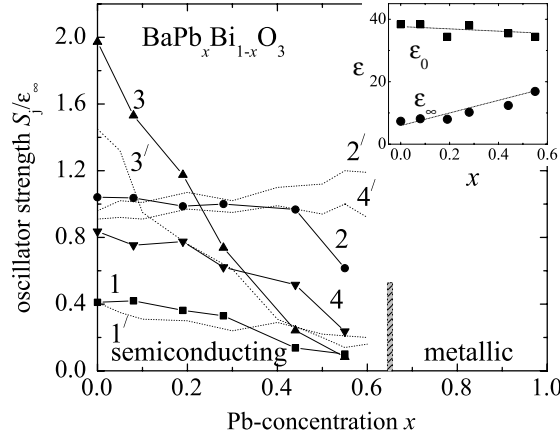


Figure 4. The compositional changes in the oscillator strength of phonon modes in $\text{BaPb}_x\text{Bi}_{1-x}\text{O}_3$. The dotted lines indicate the oscillator strength of phonon modes identified by prime numbers, as reported in [15]. The inset shows the static and high-frequency dielectric constants as a function of x . Dotted lines are a guide to eye.

In figure 4 we show compositional changes in the oscillator strength of phonon modes. The most significant feature is the remarkable decrease in the S of mode 3 with increasing x . A similar trend has been observed previously for BKBO [19], $\text{Ba}_{1-x}\text{Rb}_x\text{BiO}_3$ [36] and with differences in magnitude for BPBO [16]. The inset shows the static dielectric constant ϵ_0 and the high-frequency dielectric constant ϵ_∞ . The rapidly increasing value of ϵ_∞ means that the band-gap narrows as Pb doping increases. The ϵ_0 is estimated using a relation

$$\epsilon_0 = \epsilon_\infty + \sum S_j. \quad (2)$$

The large value of ϵ_0 that decreases with x , contrary to an increasing trend of ϵ_∞ , is clearly due to the large value of the $\sum S_j$ ($j = 1, 2, 3, 4$), which mainly decreases with Pb doping. However, in contrast to other perovskite compounds, e.g. BaTiO_3 , the giant ferroelectric S_2 is not found either in the present alloy system or in BKBO [19].

The Bi charge disproportionation mode, i.e. mode 3, which occurs due to the antiparallel motion of the neighboring Bi ions alters the bond distance between the Bi and O ions. The big change in S_3 signifies that the extent of disproportionation of charge on Bi ions is highly affected by Pb doping. We have analysed this effect quantitatively by calculating the Born effective-charge difference $2\Delta e_B^*$ and the Szigeti effective-charge difference $2\Delta e_S^*$ between inequivalent Bi sites.

The Born effective-charge difference $2\Delta e_B^*$ is estimated by the relation

$$\Delta e_B^{*2} = \frac{\mu}{4\pi N} \omega_{\text{TO}}^2(3) S_3, \quad (3)$$

where μ is the reduced mass and N is the number of Bi–Bi oscillators in the unit volume. The Szigeti effective-charge difference $2\Delta e_S^*$, which takes into account the local fields as well [37], is estimated using the relation

$$\Delta e_S^* = \frac{3\Delta e_B^*}{\epsilon_s + 2}, \quad (4)$$

where we assume that the position of Bi ions is approximately in cubic symmetry. Here $\epsilon_s = \epsilon_\infty + \epsilon_1[\omega_{\text{TO}}(3)]$, where $\epsilon_1[\omega_{\text{TO}}(3)]$ is the real part of the complex dielectric constant of all lattice vibration modes except mode 3.

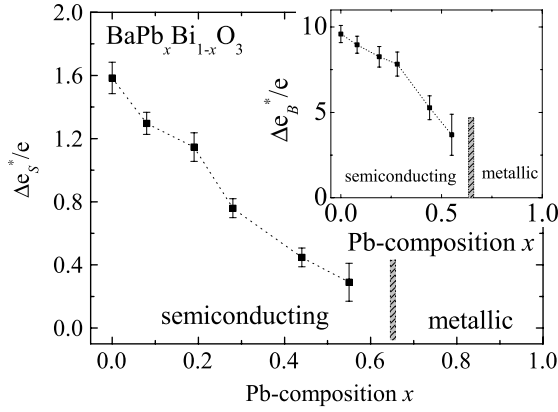


Figure 5. The compositional dependence of the Szigeti and Born (inset) effective-charge difference between inequivalent Bi sites for $\text{BaPb}_x\text{Bi}_{1-x}\text{O}_3$. Dotted lines are a guide to eye.

The compositional changes of the Δe_B^* and Δe_S^* are shown in figure 5. As mentioned above, the thermally excited carriers are almost absent at a temperature as low as 20 K. So, for $x = 0.55$, we have calculated the Δe_B^* and Δe_S^* by using the fitting parameters at 20 K, assuming that the Δe_B^* and Δe_S^* are not greatly affected by varying temperature. The Δe_S^* gives an apparent degree of ionic charge difference between inequivalent Bi ions. The maximum charge difference on the terminal BBO, in the naive framework of a purely ionic picture, is expected to be $2e$. However, we find $2\Delta e_S^* \sim 3.2e$, which is a value much larger than expected. Our estimated value is close to the $3.6e$ previously estimated by Nishio and Uwe [19] for BBO. According to the electronic structure calculation by Mattheiss *et al* and by Liechtenstein *et al* [13, 14], the maximum charge difference on the inequivalent Bi sites is as small as $0.01e$ for BBO. We therefore claim that there is definitely a strong dynamic charge transfer along the Bi–O–Bi bond length, which is varied by vibrations [38].

With increasing Pb doping, the Δe_S^* decreases monotonously and becomes almost zero as x approaches x_c , as shown in figure 5. Similar behaviour was also observed for BKBO [19]. In BPBO, the SM transition occurs when the bottom of the Pb band touches the lower Peierls Bi^{3+} band (direct energy gap) on Pb doping [5], while the ionic charge difference between inequivalent Bi sites still remains finite [24], suggesting that, even at the closing of the energy gap, the value of Δe_S^* should be non-zero, contrary to the present results. On the other hand, the indirect energy gap observed in BPBO [26–28] closes as a function of x and completely collapses on considerably large Pb doping. The observed behaviour of the vanishing of Δe_S^* is similar to, and can therefore be associated with, the behaviour of the vanishing of the indirect energy gap as x approaches x_c . These facts strongly support the idea that the SM transition should immediately occur at the value of x where the indirect energy gap closes prior to the direct gap.

It is interesting to note that the dynamically enhanced contribution of the charge difference disappears at $x_c \sim 0.65$ for BPBO and also for BKBO at $x_c \sim 0.3$ [19]. This behaviour can be related to the vanishing of the long-range order of the Bi charge disproportionation with the increase in Pb or K doping, although the short-range order persists even in the metallic region [9]. On the other hand, the disorder produced due to Pb or K doping affects the superstructure that is perceived for undoped BBO. This would eventually diminish the CDW amplitude gradually as the doping concentration increases. This is verified by the experimental observation of the gradual decrease in the oscillator strength of the disproportionation mode 3, as can typically be seen in figure 4 and also predicted theoretically [39].

Very recently, Thonhauser and Rabe [40] have reported that only the breathing distortion alone in the fcc-type cell doubling is sufficient to explain the fourth peak in the infrared (IR) spectrum. They further concluded that, although the oxygen atoms moved only a small distance of 0.04 Å along the Bi–O bond, properties such as the band gap and the Born effective charges were very sensitive to this distortion. Thus, the Born effective charge and, in turn, the Szegedi effective-charge calculations are sensitive to structural distortions and can account for Bi charge disproportionation quite accurately. The decrease in Δe_S^* with increasing Pb composition therefore demonstrates the vanishing of the amplitude of breathing distortion and, as a result, the BPBO alloy system approaches the SM transition.

4. Conclusions

We have investigated the infrared reflectivity spectra of semiconducting $\text{BaPb}_x\text{Bi}_{1-x}\text{O}_3$ using the Lorentz oscillator model. Using the oscillator strength of the Bi charge disproportionation mode, we have estimated the effective-charge difference on two inequivalent Bi sites and found a strong dynamic charge transfer enhanced by lattice vibrations. It is found that the charge difference almost vanishes as the Pb composition approaches the SM transition, in association with the closing of the indirect gap in the $\text{BaPb}_x\text{Bi}_{1-x}\text{O}_3$ system.

Acknowledgments

We thank N Nishida, the Chemical Analysis Center, for the help with EPMA. One of the authors (JA) also acknowledges the University of Tsukuba for the award of the Venture Business Laboratory foreign researchers post-doctoral fellowship for the completion of experimental work.

References

- [1] Cox D E and Sleight A W 1979 *Acta Crystallogr. B* **35** 1
- [2] Pei S, Jorgensen J D, Dabrowski B, Hinks D G, Richards D R, Mitchell A W, Newsam J M, Sinha S K, Vaknin D and Jacobson A J 1990 *Phys. Rev. B* **41** 4126
- [3] Marx D T, Radaelli P G, Jorgensen J D, Hitterman R L, Hinks D G, Pei S and Dabrowski B 1992 *Phys. Rev. B* **46** 1144
- [4] Braden M, Reichardt W, Elkaim E, Lauriat J P, Shiryaev S and Barilo S N 2000 *Phys. Rev. B* **62** 6708
- [5] Namatame H, Fujimori A, Takagi H, Uchida S, de Groot F M F and Fuggle J C 1993 *Phys. Rev. B* **48** 16917
- [6] Cox D E and Sleight A W 1976 *Solid State Commun.* **19** 969
- [7] Thornton G and Jacobson A J 1978 *Acta Crystallogr. B* **34** 351
- [8] Balzarotti A, Menushenkov A P, Motta N and Puran J 1984 *Solid State Commun.* **49** 887
- [9] Tajima S, Uchida S, Masaki A, Takagi H, Kitazawa K, Tanaka S and Sugai S 1987 *Phys. Rev. B* **35** 696
- [10] Nagoshi N, Suzuki T, Fukuda Y, Ueki K, Tokiwa A, Kikuchi K, Syono Y and Tachiki M 1992 *J. Phys.: Condens. Matter* **4** 5769
- [11] Akhtar Z N, Akhtar M J and Catlow C R A 1992 *J. Phys.: Condens. Matter* **5** 2643
- [12] Zhang X and Catlow C R A 1991 *Physica C* **173** 25
- [13] Mattheiss L F and Hamann D R 1983 *Phys. Rev. B* **28** 4227
- [14] Liechtenstein A I, Mazin I I, Rodriguez C O, Jepsen O, Andersen O K and Methfessel M 1991 *Phys. Rev. B* **44** R5388
- [15] Sleight A W, Gillson J L and Bierstedt P E 1975 *Solid State Commun.* **17** 27
- [16] Uchida S, Tajima S, Masaki A, Sugai S, Kitazawa K and Tanaka S 1985 *J. Phys. Soc. Japan* **54** 4395
- [17] Mattheiss L F, Gyorgy E M and Johnson D W Jr 1988 *Phys. Rev. B* **37** R3745
- [18] Cava R J, Batlogg B, Krajewski J J, Farrow R, Rupp L W, White A E, Short K, Peck W F and Kometani T 1988 *Nature* **332** 814
- [19] Nishio T and Uwe H 2003 *J. Phys. Soc. Japan* **72** 1274

- [20] Nishio T, Ahmad J and Uwe H 2005 *Phys. Rev. Lett.* **95** 176403
- [21] Ahmad J, Nishio T and Uwe H 2003 *Physica C* **388** 455
- [22] Ahmad J and Uwe H 2004 *Physica C* **412** 288
- [23] Ahmad J and Uwe H 2005 *Phys. Rev. B* **72** 125103
- [24] Tajima S, Uchida S, Masaki A, Takagi H, Kitazawa K, Tanaka S and Katsui A 1985 *Phys. Rev. B* **32** 6302
- [25] Takagi H, Uchida S, Tajima S, Kitazawa K and Tanaka S 1986 *Proc. Int. Conf. on Physics of Semiconductor (Stockholm)* (Singapore: World Scientific)
- [26] Uwe H and Tachibana K 1995 *Advances in Superconductivity VII* (Tokyo: Springer) p 165
- [27] Uwe H and Yamamoto Y 1996 *Proc. 7th Int. Conf. on Low Temperature Physics (Prague); Czech. J. Phys.* **46** 2689
- [28] Kozlov M E, Ji X, Minami H and Uwe H 1997 *Phys. Rev. B* **56** 12211
- [29] Shirai M, Suzuki N and Motizuki K 1990 *J. Phys.: Condens. Matter* **2** 3553
- [30] Reichardt W and Weber A W 1987 *Japan J. Appl. Phys.* **26** 1121
- [31] Braden M, Reichardt W, Ivanov A S and Rumaintsev A Y 1996 *Europhys. Lett.* **34** 531
- [32] Brodsky M H, Lucovsky G, Chen M F and Plaskett T S 1970 *Phys. Rev. B* **2** 3303
- [33] Lobo R P S M and Gervais F 1996 *Solid State Commun.* **98** 61
- [34] Takahashi Y, Ji X, Nishio T, Uwe H and Ohshima K 2002 *J. Phys.: Condens. Matter* **14** 5477
- [35] Cox D E and Sleight A W 1976 *Proc. Conf. on Neutron Scattering* (Springfield, VA: National Technical Information Service)
- [36] Inoue A, Iyo A, Uwe H, Sakudo T, Tanaka Y and Tokumoto M 1992 *Adv. Supercond.* **4** 139
- [37] Szigeti B 1949 *Trans. Faraday Soc.* **45** 155
- [38] Harrison W A 1980 *Electronic Structure and the Properties of Solids: The Physics of the Chemical Bonds* (San Francisco, CA: Freeman)
- [39] Prelovsek P, Rice T M and Zhang F C 1987 *J. Phys. C: Solid State Phys.* **20** L229
- [40] Thonhauser T and Rabe K M 2006 *Phys. Rev. B* **73** 212106